out, however, that no correction for $E\times B$ drifts has been made, because the plasma potential is not known for these discharges.

Attempts were made to compare the experimental results with the predictions for the $m=1$ internal kink mode.[4,5] Pictures like Fig. 3 suggest an experimental growth rate $\gamma\approx 3\times 10^3$ sec^{-1}. The theoretical linear growth rate depends on the exact radial dependence of q. For parabolic temperature profiles ($n_e=$const, $j\sim T_e^{3/2}$) we derive from Eq. (13) of Ref. 5

$$\gamma_{\rm theor}=\tfrac{2}{3}\pi(v_A/R)(\beta_{z0}+\tfrac{1}{2}r_s^2/R^2),$$

where v_A is the Alfvén velocity, R the major radius, β_{z0} the toroidal β in the center of the column, and r_s the radius of the singular surface ($q=1$). This formula gives a value of $\gamma_{\rm theor}$ equal to 2×10^4 sec^{-1}, which is larger than the experimental growth rate by a factor of about 7.

We can also compare the radial profile of the oscillation amplitude [Fig. 2(d)] with the prediction for the internal kink mode, i.e., displacement $\xi=$const for $r<r_s$ and $\xi=0$ for $r>r_s$. The x-ray signal is the integral over the x-ray sources along a line of sight. To obtain the x-ray radial profile a set of scans at different lines of sight have been inverted. Without going into the details, we state that the shape of the profile is in reasonable agreement with the theoretical prediction. The experimental displacement ξ, however, seems to be larger than the predicted nonlinear displacement of Ref. 5 by approximately an order of magnitude. Experimentally we obtain $\xi/r_s\approx 0.2$. It should be pointed out that resistivity is not included in the present theory and that it is likely that a tearing-mode version of this instability exists (Ref. 5, p. 1899) which might lead to smaller growth rates and larger displacements.

The technical assistance of W. Mycock and the ST tokamak operating crew is gratefully acknowledged. We thank Dr. K. Bol, Dr. H. P. Furth, and Dr. P. Rutherford for valuable discussions.

*This work was supported by the U. S. Atomic Energy Commission under Contract No. AT(11-1)-3073.

[1]S. von Goeler, W. Stodiek, H. Eubank, H. Fishman, S. Grebenshchikov, and E. Hinnov, "Thermal X-Ray Spectra and Impurities in the ST Tokamak" (to be published).

[2]V. A. Vershkov, C. E. Lisenko, I. B. Semenov, and A. T. Scherbac, Kurchatov Institute Report No. IAE-2291, 1973 (unpublished), and Princeton University Plasma Physics Laboratory Report No. MATT-TRANS-112, 1974 (unpublished).

[3]R. R. Smith, Princeton University Plasma Physics Laboratory Report No. TM-273, 1974 (unpublished).

[4]V. D. Shafranov, Zh. Tekh. Fiz. 40, 241 (1970) [Sov. Phys. Tech. Phys. 15, 175 (1970)].

[5]M. N. Rosenbluth, R. Y. Dagazian, and P. H. Rutherford, Phys. Fluids 16, 1894 (1973).

Adiabatic Compression of Plasma Vortex Structures*

D. R. Wells, E. Nolting, F. Cooke, Jr., J. Tunstall, P. Jindra, and J. Hirschberg
Department of Physics, University of Miami, Coral Gables, Florida 33124
(Received 3 June 1974)

Plasma vortex structures generated by conical theta-pinch guns have been successfully compressed and amplified by secondary adiabatic compression. A pair of vortex rings meet at the center of a primary magnetic mirror. A secondary mirror starts to compress them as soon as the collision has occurred. Peak ion temperatures of 170 eV have been obtained at an $n\tau$ of 10^{12} sec/cm^3 by utilizing a capacitor bank that stores 250 kJ.

Over the past fourteen years, an extensive series of experiments concerned with naturally occurring stable plasma states has been performed.[1-6] We have intensively studied, both theoretically and experimentally, a whole new field of plasma physics concerned with the problem of production, heating, and application of these states.

A theory has been developed which predicts a spectrum of naturally occurring stable states.[5,7,8] The particular stable state studied at the University of Miami consists of a closed plasma structure produced by conical theta-pinch guns. This state is the force-free collinear vortex ring or spheroid first described by Wells.[1,2]

It has been shown elsewhere that, by variational methods, one can predict the current and mass-flow patterns of the stable states of lowest free energy.[5,7,8] These structures, or plasma cells, have minimal free energy available for driving instabilities and thus can persist for long periods of time, even when they are violently perturbed by the surrounding plasma and electromagnetic fields. An important part of this work is concerned with the inclusion of the mass-flow terms in the equation of motion of the plasma.[5,8] The most stable plasma states are structures with a large part of their total energy in the form of mass-flow energy. Some of these properties of the cells have been extensively investigated by others, and the results obtained verify in detail the results of Wells, Jones and Miller,[9] Turner,[10] and Small and Bostick.[11]

Difficulties have been encountered in the past in attempting to couple the primary currents in the conical theta-pinch guns to the secondary currents in the plasma rings. The rings move away from the guns so fast that the coupling coefficient decreases rapidly and the rings move away before much energy has been transferred to them. This problem has been overcome by abandoning the attempt to couple a very big capacitor bank directly to the rings.[4] Instead, a set of rings originating at each end of a primary magnetic mirror are produced in and guided by a steady-state mirror field (dc mirror coils shown in Fig. 1) to the center of the machine. The ring moving parallel to the mirror field has its velocity and magnetic fields antiparallel (contrarotational). The ring moving antiparallel to the primary mirror field has its velocity and magnetic fields parallel (corotational). Both rings are force free [e.g., $\vec{j}\times\vec{\beta}=0$ and $(\nabla\times\vec{v})\times\vec{v}=0$. Thus, the contrarotational ring is right handed in $B_\theta+B_p$ and the corotational ring is left handed in $B_\theta+B_p$, where B_θ is the toroidal component of the trapped magnetic induction field in the rings and B_p is the corresponding trapped poloidal field.[3,4,12] They then collide and are amplified and compressed by a secondary mirror system located at the center of the primary mirror system. The current flow in the secondary compression coils is in the same direction as the currents flowing in the primary-mirror coils. Thus (by Lenz's law) they both compress the vortex rings and amplify their currents. The diamagnetic currents in the rings increase as the current in the secondary compression coils increases. The toroidal currents in the two rings are in the same direction. The poloidal-current components are in opposite directions. The ring currents are left-handed and right-handed helices. This geometry is illustrated in Fig. 1. The cylindrical vacuum chamber has an 8 in. outside diameter. The centerline distance between the compression coils is 12 in.

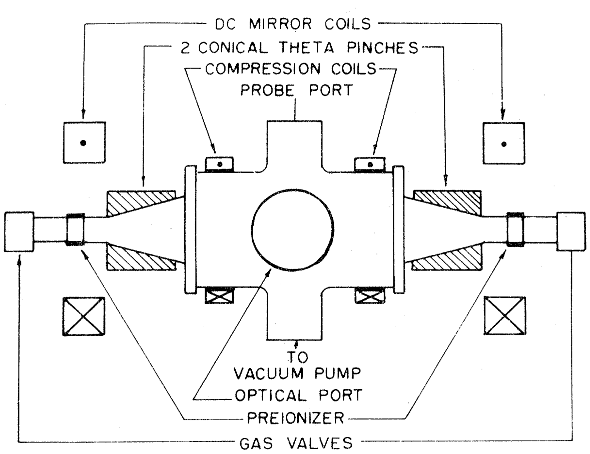

FIG. 1. Schematic diagram of machine used for secondary compression of plasma vortex structures. Primary-mirror field strength was 900 G.

The base pressure in the vacuum system is 3×10^{-6} Torr. Deuterium gas is admitted by the pulsed gas valves. The operation of these valves is described in detail in Ref. 12. The preionizers consist of a set of conical arc guns which strike an arc in the gas when it drifts into the preionizer region of the chamber. The effective gas pressure in the preionizers is 40 mTorr.

The conical theta pinches are powered by a single General Electric "clamshell" capacitor rated at 1 μF, 50 kV. The quarter-cycle rise time on the conical theta pinches is 0.5 μsec. They ring out in 3 μsec. The peak magnetic fields in the throats of the conical theta-pinch guns were 20 kG at 18 kV. The secondary compression coils are powered by a $\frac{1}{4}$-MJ capacitor bank consisting of a series-parallel combination of 15-μF capacitors rated at 20 kV. This bank and its operations are described elsewhere.[12] The current rises to a peak value in 19.6 μsec. A crowbar is activated at peak current. The decay time for the circuit is 30 μsec. The peak magnetic field produced by the secondary compression coils is 35 kG at 20 kV. The bank was not fired at voltages over 15 kV because of crowbar-switching difficulties at higher voltages.

Since the rings, after collision, are stationary in the laboratory frame, the coupling problem is no longer critical and very large currents and mass motions can be induced in the double-ring system. The macroscopic toroidal conduction currents in the rings produce a long-range attraction force which draws them together; the vortex forces (mass-flow forces) and poloidal conduction currents (which are strongest near the surface of the rings and produce a short-range force) force them apart.[4,6,12,13] Thus, they oscillate axially at the center of the primary mirror when the secondary mirror is applied. This oscillation has been observed in earlier experiments without secondary compression. We observe the same characteristic streak pictures of these phenomena when the secondary compression is applied.

There is no apparent limit to the size of the currents that can be induced or the amount of compression that can be obtained without producing any instability in the rings (see Fig. 2). The compression mirror acts as its own magnetic containment bottle and no special auxiliary fields are required. Currents as high as 120 kA have been induced in rings compressed to 2 cm major diameter. In earlier experiments[4,6] the induced ring currents were measured directly with Rogowski coils. In the very-high-field experiments described here, the ring currents are calculated by the use of the coupling coefficients between the compression coils and the current rings which were calculated from earlier direct measurements.[12] There is no change in these coefficients at the higher field levels since the ring separation and oscillation as observed by streak pictures do not change at higher field levels. These phenomena depend directly on the coupling coefficients.

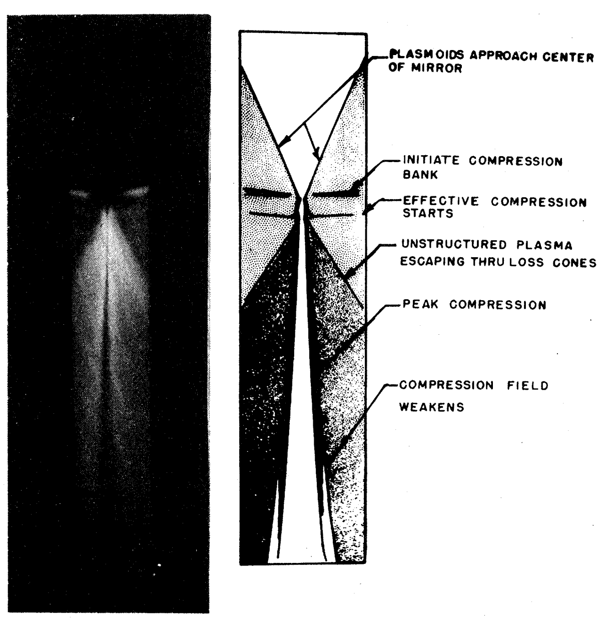

FIG. 2. Streak picture and schematic diagram illustrating collision of vortex structures at center of secondary mirror system. Time goes from top to bottom of the picture and diagram. Streak time is 50 μsec. The horizontal slit was placed along the centerline of the machine, between the secondary compression coils.

Thermalization of the macroscopic currents and mass motions can be accurately controlled. Thermalization begins when the compression field becomes high enough to overcome the short-range repulsive forces that hold the rings apart. The macroscopic flow energy and the energy trapped in the rings by conduction currents is then turned into random thermal energy as the rings slowly decay. The ring decay rate is a function of mirror ratio and the time that the compression field remains at values high enough to contain the high-temperature plasma. The ion temperatures reported below were obtained at peak secondary compression before the rings thermalized and formed a normal mirror plasma. Complete flow breakdown and thermalization has not occurred in the compression shown in Fig. 2. This streak picture was taken for a compression at relatively low voltage for the purpose of a clear picture of the event.

Classical diffusion of plasma held in the mirror but not in the rings can be observed, but the plasma trapped in the rings remains in the system for times that are orders of magnitude greater than those predicted for classical mirror diffusion. These decay rates can be easily computed from streak pictures of the type illustrated in Fig. 2.

The rings reduce the magnetic field at the center of the mirror system by 80% and constitute a "plugged" open-ended system which is stable and has small end losses.

Measurements of the ion temperature by observation of Doppler broadening in a deuterium plasma for various voltages on the compression-coil capacitor bank have been made by using a multichannel Fabry-Perot interferometer[13] especially developed for the purpose. Since the bank is switched by air-gap switches, one would expect that switch efficiency would increase rapidly with increasing bank charging voltages. The voltage drop across the gap is approximately 3.0 kV at 9 kV bank voltage. It decreases rapidly to a fraction of a kilovolt at 14 kV. The switch loss

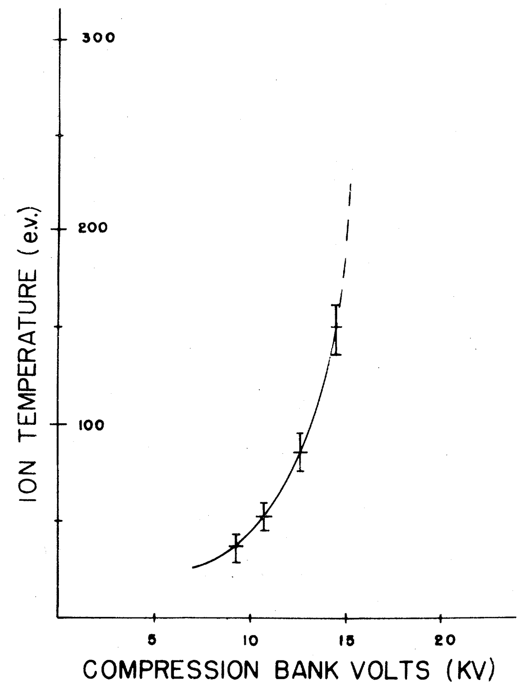

FIG. 3. Ion temperature of deuterium versus voltage applied to capacitor bank that powers the secondary-mirror coils. The temperatures were measured with a Fabry-Perot interferometer.

is the product of the voltage and switch current. At low bank voltages, this is an appreciable fraction of total bank voltage. At high voltages it is not. Thus, the maximum magnetic field is a nonlinear function of bank voltage. The peak temperatures should increase more rapidly than the square of the voltage. Figure 3 shows the results of these measurements. Ion temperatures of 170 eV have been observed at 14.3 kV on the 20-kV capacitor bank. It should be emphasized that this is a slow bank with a quarter-cycle rise time of 19.6 μsec. Appropriate corrections have been made for instrument broadening, macroscopic motion of the plasma, turbulence effects, and pressure broadening.[13,14]

Ion density was measured by scanning the D_β line at 4861 Å. Peak density at 14.3 kV on the compression bank was 10^{16} ions/cm^3. Observed oscillations in density at the center of the machine are in phase with the axial oscillation of the rings observed in the streak pictures (Fig. 2). Electron temperature at 8 kV on the compression bank was measured by taking line-intensity ratios of He II at 4686 Å and He I at 5875 Å. At peak compression, the ion temperature is 30 eV and the electron temperature is approximately 10 eV. There is preferential heating of the ions during secondary compression.

Peak temperatures and densities persist for times of the order of 20 μsec. No attempt has yet been made to optimize the magnetic mirror ratio of the compression mirror. The data were taken with a secondary-mirror ratio of 1.4. There are strong theoretical reasons to believe that this ratio must be increased to at least 3.5 for optimum containment of the rings during compression.

We note that for operation at a mirror ratio of 1.4, $n\tau \cong 10^{12}$, $T_i = 170$ eV, at 14.3 kV on the compression bank.

The authors gratefully acknowledge useful discussions with Dr. Joseph Mather, Dr. James Phillips, and Dr. Joseph Di Marco of the Los Alamos Scientific Laboratories and Mr. Marvin Young of the Naval Research Laboratories.

*This work was supported by the U. S. Air Force Office of Scientific Research under Grant No. 72-2295 and the National Science Foundation under Grant No. GP-43733.

[1]D. R. Wells, Phys. Fluids 5, 1016 (1962).
[2]D. R. Wells, Phys. Fluids 7, 826 (1964).
[3]D. R. Wells, Phys. Fluids 9, 1010 (1966).
[4]D. R. Wells and J. Norwood, Jr., Phys. Fluids 3, 21 (1969).
[5]D. R. Wells, J. Plasma Phys. 4, 645 (1970).
[6]E. Nolting, P. Jindra, and D. R. Wells, J. Plasma Phys. 9, 1 (1973).
[7]D. R. Wells and J. Norwood, Jr., Phys. Fluids 11, 1582 (1968).
[8]D. R. Wells, University of Miami Report No. MIAPH-PP-70.13, 1971 (unpublished).
[9]W. B. Jones and R. D. Miller, Phys. Fluids 11, 1550 (1968).
[10]R. Turner, Phys. Fluids 13, 2398 (1970).
[11]R. L. Small and W. H. Bostick, Grumman Aircraft Engineering Corporation, Research Department, Report No. RE-284, 1967 (unpublished).
[12]E. Nolting, U. S. Air Force Office of Scientific Research Scientific Report No. AFOSR-TR-71-2905 (unpublished).
[13]F. N. Cooke, Jr., thesis, University of Miami, 1974 (unpublished).
[14]J. Hirschberg, private communication.

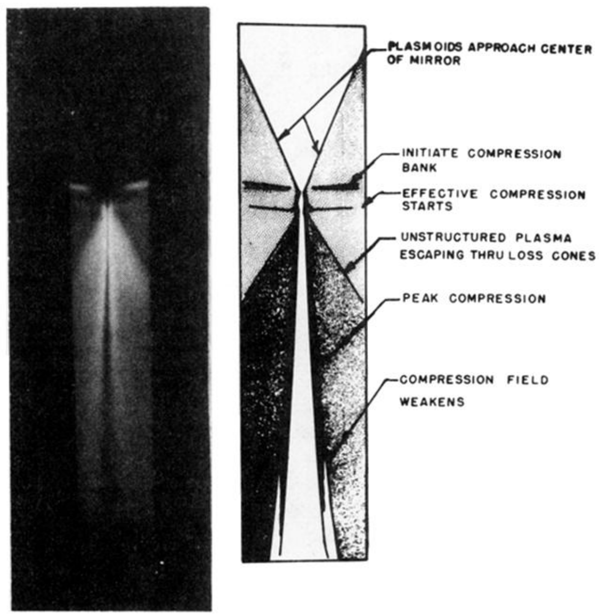

FIG. 2. Streak picture and schematic diagram illustrating collision of vortex structures at center of secondary mirror system. Time goes from top to bottom of the picture and diagram. Streak time is 50 μsec. The horizontal slit was placed along the centerline of the machine, between the secondary compression coils.